

1 **Title: Making sense of virus size and the tradeoffs shaping viral fitness**

2 Running title: Tradeoffs shaping virus size

3

4 Authors: Kyle F. Edwards^{*1,2}, Grieg F. Steward^{1,3}, Christopher R. Schvarcz^{1,4}

5 ¹Department of Oceanography, University of Hawai‘i at Mānoa, Honolulu, HI

6 ²kfe@hawaii.edu, ³grieg@hawaii.edu, ⁴schvarcz@hawaii.edu

7 *corresponding author address: 1000 Pope Rd, Honolulu, HI 96822, phone: 808-956-6198, fax:

8 808-956-9225

9

10 Keywords: giant virus, allometric scaling, host range, burst size, diffusivity, decay rate,
11 competition, phytoplankton, bacteria, phage

12 Article type: Reviews and Syntheses

13 Abstract word count: 200

14 Main text word count: 6708

15 Number of references: 83

16 Numbers of figures / tables / text boxes: 4 / 0 / 0

17

18 Authorship statement: All authors contributed to the conception and outline of the work. K.F.E wrote
19 the initial manuscript, analyzed mathematical models, and contributed to data compilation and
20 analysis. G.F.S and C.R.S. both contributed to manuscript writing and to data compilation and
21 analysis.

22

23 Data accessibility statement: Should the manuscript be accepted, the data supporting the results will be
24 archived in an appropriate public repository and the data DOI will be included at the end of the article.

25 **Abstract**

26 Viruses span an impressive size range, with genome length varying a thousandfold and
27 virion volume nearly a millionfold. For cellular organisms the scaling of traits with size is a
28 pervasive influence on ecological processes, but whether size plays a central role in viral ecology is
29 unknown. Here we focus on viruses of aquatic unicellular organisms, which exhibit the greatest
30 known range of virus size. We develop and synthesize theory, and analyze data where available,
31 to consider how size affects the primary components of viral fitness. We argue that larger viruses
32 have fewer offspring per infection and slower contact rates with host cells, but a larger genome
33 tends to increase infection efficiency, broaden host range, and potentially increase attachment
34 success and decrease decay rate. These countervailing selective pressures may explain why a
35 breadth of sizes exist and even coexist when infecting the same host populations. Oligotrophic
36 ecosystems may be enriched in “giant” viruses, because environments with resource-limited
37 phagotrophs at low concentrations may select for broader host range, better control of host
38 metabolism, lower decay rate, and a physical size that mimics bacterial prey. Finally, we
39 describe where further research is needed to understand the ecology and evolution of viral size
40 diversity.

41

42

43

44

Introduction

45

46 Viruses are ubiquitous and abundant molecular symbionts that influence individual health,
47 population and community dynamics, evolution, and biogeochemistry, across the tree of life.
48 By nature, viruses are smaller than the cells they infect, but the range of virus sizes is nonetheless
49 substantial, with lengths of viral particles (virions) varying from 17 nm to ~1.5 μm , and genome
50 size varying from ~1 kb to 2.5 Mb (Campillo-Balderas et al. 2015). The largest 'giant' viruses
51 have primarily been isolated from unicellular protists (Campillo-Balderas et al. 2015, Wilhelm
52 et al. 2017), although there is metagenomic evidence for 'megaphages' of prokaryotes with
53 genomes up to 716 kb (Devoto et al. 2019, Al-Shayeb et al. 2020), and a chaetognath appears
54 to be infected by viruses 1.25 μm in length (Shinn and Bullard 2018). In contrast, the known
55 viruses of plants and fungi have genomes < 30 kb (Campillo-Balderas et al. 2015). At a finer
56 phylogenetic scale, particular species or strains of prokaryotes and eukaryotes can be infected
57 by viruses of very different size. For example, the marine bacterium *Cellulophaga baltica* is
58 infected by phages ranging from 6.5 to 242 kb (Holmfeldt et al. 2007) and the marine
59 dinoflagellate *Heterocapsa circularisquama* is infected by a 4.4 kb ssRNA virus and a 365 kb
60 dsDNA virus (Tomaru et al. 2009).

61 For cellular life, body size is a 'master trait' that influences numerous organismal properties,
62 such as metabolic rate, nutrient uptake affinity, predator-prey linkages, and population growth
63 rate (Finkel 2001, Brown et al. 2004, Fuchs and Franks 2010, Edwards et al. 2012). The
64 substantial variation in virus size raises the question of whether size plays a similar central role
65 in virus ecology and evolution (Record et al. 2016). For example, are there general relationships
66 between virus size and key viral traits? Do size-related tradeoffs lead to selection for different
67 sizes of viruses infecting different kinds of hosts, or under different environmental conditions?

68 How do viruses of different size coexist when infecting the same host population? There are
69 straightforward physical reasons why being smaller should be advantageous for a virus: smaller
70 particles should encounter hosts faster due to greater diffusivity, at least in aquatic systems or
71 aqueous microenvironments, and limited host resources during infection can be partitioned
72 among a greater number of 'offspring'. The existence of a spectrum of virus sizes implies that
73 the costs of increased size can be offset by countervailing benefits. Virion size and genome size
74 are tightly correlated (Cui et al. 2014), and benefits of increased size likely derive from the
75 functions encoded by viral genes, including better control of attachment to the host, replication,
76 transcription, translation, and host metabolism; strategies countering host antiviral defenses; and
77 repair of damaged viral nucleic acids (Sharon et al. 2011, Samson et al. 2013, Fischer et al.
78 2014, Koonin and Yutin 2019, Mendoza et al. 2019). These functions could increase the
79 probability of successful infection, the number of virions produced per infection, the range of
80 hosts than can be successfully infected, and/or the persistence of virions in the extracellular
81 environment.

82 In this study, we focus on the question of how virus size affects key viral traits, and how
83 these traits affect viral fitness. We develop and summarize relevant theory, synthesize and
84 analyze available data, and outline major knowledge gaps and future research directions. We
85 focus primarily on viruses that infect aquatic microbes (unicellular prokaryotes and eukaryotes),
86 as these viruses are known to vary greatly in size and have been relatively well-studied in culture.
87 However, most of the concepts we develop should be useful for understanding viruses in general.

88

89

Theory for how viral fitness is determined by key viral traits

90

91

92

93

94

95

96

97

98

99

100

101

102

In order to connect a metric of fitness to virus traits (burst size, latent period, contact rate, decay rate, etc.) we imagine a lytic virus population that may compete for hosts with one or more additional virus populations. Using a simple model of virus-microbe population dynamics, at steady state the density of the limiting resource, uninfected cells, is $S^* = \frac{d}{k(be^{-mL}-1)}$ (eqn. 1; Appendix S1). Here S is the density of uninfected cells, m is the host mortality rate from causes other than viral infection, b is the burst size (new virions produced per infection), L is the latent period, d is the viral decay rate, and k is the effective adsorption rate—the rate at which successful new infections are formed. The parameter k can be decomposed into subprocesses, and here we define $k = caw$, where c is the contact rate at which host and virus encounter each other, a is the attachment efficiency (probability that encounter leads to successful attachment), and w is the probability that attachment leads to a successful infection (eventual lysis of the host, releasing new virions). The distinction between contact rate and attachment efficiency will be important when considering the role of virus size.

103

104

105

106

107

108

109

110

The quantity S^* is the uninfected host density at which growth of the viral population balances the decay rate. Therefore, this is also the host density threshold required for persistence of a viral population, and if the host density is initially greater it will be cropped down to this level at steady state. S^* can be used as a measure of viral fitness because if there are two viral strains, and $S_1^* < S_2^*$, then strain 1 will drive the host to a lower density and competitively exclude the other strain at equilibrium (Tilman 1982). It is more intuitive to consider the inverse of S^* as a metric of fitness, because a smaller S^* equates to greater competitive ability; the inverse of S^* is $\frac{k(be^{-mL}-1)}{d}$. This quantity is the average net number of new virions produced per

111 infection ($be^{-mL} - 1$), scaled by the rate of successfully encountering a new host (k) relative to
112 the rate of 'dying' while waiting to encounter a new host (d). This analysis assumes that host-
113 virus dynamics reach a steady-state attractor, which may not be true, but the S^* quantity is still
114 a useful index of competitive ability. Furthermore, in a simpler model with no latent period it
115 can be shown that S^* predicts the winner in competition even if populations fluctuate (Appendix
116 S2). This analysis relates traits to fitness for lytic viruses, which we focus on in this study due to
117 a greater accumulation of relevant trait data, but potential effects of size on viruses with
118 temperate strategies will be discussed as well.

119 In Appendix S3 we extend this analysis to ask under what conditions a broader host range
120 is selected for. The main result is that fitness (measured in terms of competitive outcomes) is
121 proportional to host range (measured as the number of host strains that can be infected). This
122 means that a generalist virus and a specialist virus will have similar fitness when the cost of
123 generalism is directly proportional to host range breadth. For example, if a generalist virus can
124 infect twice as many strains as specialist viruses, but has an adsorption rate that is 50% lower
125 on each strain, it will be competitively equivalent to the specialists. If the cost of generalism is
126 lower then generalism will be favored, and vice versa. These results are derived from a simple
127 model but they allow us to quantify, as a first approximation, how tradeoffs involving host range
128 and other viral traits may affect selection on virus size.

129

130 **How does virus size affect contact rate and attachment to host cells?**

131 We now consider key viral traits individually, to outline expectations for how virus size
132 may affect each trait and analyze relevant data where it is available. Adsorption rate is important

133 for viral fitness (eqn. 1) because it determines the rate at which new infections can be established,
134 as well as the time a viral particle spends in the extracellular environment where it may be
135 exposed to UV radiation, adsorption to non-host material, ingestion, etc. (Suttle and Chen 1992,
136 Noble and Fuhrman 1997). As described above, it is useful to separate the adsorption rate into
137 the contact rate c (per capita rate at which hosts and viruses encounter each other) and the
138 attachment efficiency a (probability of successful attachment to the host). In theory the contact
139 rate will depend on physical processes of Brownian motion, advection, and turbulence, while
140 attachment efficiency will be a function of host receptor availability, affinity of the receptor for
141 the virus, and mechanisms such as reversible binding by viral fibers that keep the virus from
142 diffusing away from the host (Schwartz 1976, Wickham et al. 1990, Storms and Sauvageau
143 2015).

144 Physical theory for contact rate typically starts by asking what the rate would be if viruses
145 relied solely on molecular diffusion to encounter their hosts, and if all viruses that contact the
146 host are adsorbed. Under pure diffusion the contact rate is predicted to be:

$$147 \quad c = 4\pi r_H D_V \quad (2)$$

148 where r_H is host radius and D_V is the diffusivity of the virus (Murray and Jackson 1992). The
149 diffusivity of a spherical virus is predicted to be:

$$150 \quad D_V = \frac{k_B T}{6\pi\eta r_V} \quad (3)$$

151 where k_B is the Boltzmann constant, T is temperature, η is dynamic viscosity of water, and r_V is
152 the virion radius. Therefore, the diffusion-limited contact rate is predicted to be inversely
153 proportional to virus diameter, which is a substantial fitness cost of increasing size.

154 The diffusivity of viruses due to Brownian motion is low enough that contact rates could
155 be increased considerably by processes that create fluid motion relative to the host cell. Rates
156 of diffusion can be enhanced by advective flow arising from host motility, feeding currents, or
157 host sinking, and diffusion can also be enhanced by turbulence, which causes shear around the
158 host cell (Murray and Jackson 1992). Host motility, feeding currents, sinking, and turbulence
159 can also lead to the host cell encountering the virus by direct interception (i.e., without the aid
160 of Brownian motion), which is the mechanism by which small flagellates are thought to
161 encounter immotile prey (Shimeta 1993, Kiørboe 2008).

162 The results in Appendix S4 show that diffusion enhanced by advection is the primary
163 mechanism that could significantly increase virus contact rates beyond the ‘pure diffusion’
164 scenario (eqn. 2), and so we consider here how that mechanism depends on virus size. An
165 approximate formula for contact rate when advection enhances diffusion is:

$$166 \quad c = 4\pi r_H D_V 0.5 \left[1 + \left(1 + 2 \frac{u_H r_H}{D_V} \right)^{1/3} \right] \quad (4)$$

167 where u_H is the velocity of the host relative to the surrounding water (Murray and Jackson 1992).

168 Because the formula includes the term $\left(1 + 2 \frac{u_H r_H}{D_V} \right)^{1/3}$, the enhancement of contact rates due to
169 advection is greater as u_H and r_H increase, and also as r_V increases (because D_V is in the
170 denominator, and $D_V \sim 1/r_V$). In other words, host motility matters more for bigger hosts, for
171 hosts that swim faster, and for bigger, less diffusive viruses. These effects are visualized in Fig.
172 1A, which shows that contact rate always declines with virus size, but the penalty for large size
173 is slightly less when hosts are motile. The effect of host motility on contact rates ranges from
174 modest (~2-fold increase for a 20 nm virus infecting a 1 μm host swimming at 30 $\mu\text{m s}^{-1}$) to large
175 (>10-fold increase for a 300 nm virus infecting a 20 μm host swimming at 250 $\mu\text{m s}^{-1}$). Langlois

176 et al. (2009) use numerical simulation to show that the effect of swimming on diffusion may be
177 underestimated by the formulas used here, but the effect is only ~2-fold for the relevant particle
178 sizes and swimming speeds.

179 Although Brownian motion, potentially enhanced by advection, is expected to drive
180 contact rates, it is possible that direct interception is important for particularly large viruses
181 encountering hosts that generate a strong current (Figs. S1-2). The simple model of interception
182 based on Stokes flow may underestimate particle contact rates (Langlois et al. 2009), and if
183 interception is great enough then 'giant' viruses could have greater contact rates than slightly
184 smaller viruses (Figs. S1-2). Therefore, a better understanding of the physics of particle encounter
185 will be important for understanding virus ecology and size evolution, in addition to
186 understanding predator-prey dynamics among microbes.

187 We have compiled published data on the adsorption rates of viruses of aquatic microbes
188 (cyanobacteria, heterotrophic bacteria, eukaryotic phytoplankton, heterotrophic protists; Table
189 S1; Methods S1) to ask whether virus size has any relation to contact rate or attachment
190 efficiency. There is a tendency for adsorption rate to be greater for larger viruses (Fig. 1B), but
191 this may be due to larger viruses having hosts that are larger, more motile, or both. We therefore
192 used eqns. 2-4 to ask how observed adsorption rates compare to the theoretical maximum (Fig.
193 1C). Predictions and observations are positively correlated ($r = 0.68$), but many of the
194 observations are 10-100x lower than predicted. This is consistent with a previous analysis of
195 adsorption rates of phages (Talmy et al. 2019) and could be due to sparse host receptors, a low
196 binding affinity of the virus ligand to the host receptor, or a lack of mechanisms for keeping the
197 virus from diffusing away from the host before irreversible binding to the receptor occurs (Storms
198 and Sauvageau 2015). Several of the large eukaryotic viruses have adsorption rates that are

199 higher than the prediction based on Brownian motion alone (eqn. 2), but accounting for host
200 swimming (eqn. 4) brings them closer to the 1:1 line (Fig. S3). However, a number of the phages
201 also have motile hosts, and including reasonable numbers for host swimming speed moves them
202 further below the 1:1 line (Fig. S3).

203 Fig. 1D shows the proximity of adsorption rate to the theoretical maximum as a function
204 of virus size. Although the sample size is limited, it is noteworthy that the five largest viruses are
205 all fairly close to the theoretical maximum. It is possible that some of the functions encoded in
206 larger genomes increase attachment efficiency, such as the synthesis of proteins that aid
207 attachment to host glycans (Rodrigues et al. 2015), or a greater diversity of proteins for binding
208 host receptors (Schwarzer et al. 2012). If attachment efficiency is promoted strongly by certain
209 genes, this could outweigh the reduction in diffusivity associated with larger size, increasing the
210 actual adsorption rate. If a virus is large enough to induce phagocytosis this could also
211 potentially increase encounter efficiency relative to other mechanisms of entry, and some of the
212 largest viruses have been shown to enter their amoeba hosts via phagocytosis (Rodrigues et al.
213 2016). If phagocytosis is in fact a more efficient entry mechanism then large size could be
214 selected for, in order to induce phagocytosis (Rodrigues et al. 2016). Protists that eat bacteria-
215 sized prey are known to ingest larger prey at higher rates, which could be due to differences in
216 contact rates or size preferences during ingestion (Chrzanowski and Šimek 1990, Holen and
217 Boraas 1991, Šimek and Chrzanowski 1992, Epstein and Shiaris 1992). Additional
218 measurements of adsorption rates for viruses across the full size spectrum will be needed to test
219 whether larger size is on average an advantage or disadvantage, and whether rates of successful
220 encounter and infection differ for viruses that enter by phagocytosis.

221

222
223
224
225
226
227
228
229
230
231
232
233
234
235
236
237
238
239
240
241
242
243
244

How does virus size affect viral production during infection?

Burst size and latent period of a lytic virus are determined by the rate at which new virions are created during an infection and the timing of cell lysis (You et al. 2002). The production of virions may decline as host resources are depleted, and the timing of cell lysis may evolve in response to intracellular conditions, host density, and other factors (Wang et al. 1996, Abedon et al. 2003). A previous analysis of phytoplankton viruses showed that burst size of dsDNA viruses may be limited by the host resources used in virus genome replication, with lysis occurring once those resources are exhausted (Edwards and Steward 2018). By contrast, small ssDNA and ssRNA viruses that infect large hosts may maximize fitness by lysing the host before those resources are exhausted (Edwards and Steward 2018).

In light of these results, we focus here on the role of viral genome size in constraining burst size and the rate of viral replication. Eqn. 1 shows that burst size and latent period are expected to play a large role in virus fitness, and therefore viral size evolution may be driven in part by its effects on these life history parameters. We previously showed that burst size is correlated with the host:virus genome size ratio (Edwards and Steward 2018), and this relationship can be decomposed into the effects of host genome size and virus genome size (Methods S1; Table S2). Of the total variation in burst size across phytoplankton viruses, 48% is explained by host and virus genome sizes in combination, with a partial R^2 of 30% for host genome size and a partial R^2 of 14% for virus genome size (4% of variation cannot be uniquely attributed to either predictor because host and virus genome sizes are partially correlated). Although burst size tends to decline for larger viruses, the effect of virus genome size is less than proportional, i.e., a tenfold increase in genome size leads to a less than tenfold decrease in burst size (Fig. 2A). The estimated slope for virus genome size is -0.52 (95% CI =[-0.225, -0.911]) when host and

245 virus taxonomy are included as random effects, or a slope of -0.3 (95% CI = [-0.11, -0.55]) when
246 host and virus taxonomy are not included. This means that a tenfold increase in virus genome
247 size would be expected to reduce burst size by a factor of $1/10^{-0.52} = 3.3$ or $1/10^{-0.3} = 2.0$.

248 A less-than-proportional relationship between virus genome size and burst size suggests
249 that larger viruses are producing more total viral material per infection, which could happen if
250 viruses with larger genomes are better at extracting resources from their hosts, better at
251 maintaining metabolic processes that fuel replication, more efficient at transcription or
252 translation, etc. For another perspective on the same processes we can consider how quickly
253 new virions are produced during an infection. All else equal, we would expect that larger virions
254 take longer to construct, due to rate limitation by protein elongation, supply of amino acids or
255 dNTPs, or other processes (You et al. 2002, Birch et al. 2012). The data for phytoplankton viruses
256 exhibit a weak trend of virion production rate declining with virus size ($F_{1,36} = 2.3$, $p = 0.14$; Fig.
257 2B), which is consistent with a penalty for larger size that is not directly proportional to size.
258 Finally, rather than looking at production rate on a per virion basis we can consider production
259 rate on a per nucleotide basis, to quantify the total rate at which viral nucleotides are produced
260 during an infection. Nucleotide production rate increases strongly with viral size, with the
261 largest viruses on average producing viral nucleotides ~100x faster than the smallest viruses (Fig.
262 2C; $F_{1,11} = 6.5$, $p = 0.027$). In combination with Fig. 2A-B, this argues that larger size does incur
263 a cost of producing fewer offspring per infection, but that the cost is partially mitigated by a
264 more effective infection process facilitated by the functions encoded in larger genomes.
265 Repeating these analyses using virion volume instead of genome size produces similar results,
266 but the slope of burst size vs. virus genome size is shallower (a 10-fold increase in virion volume
267 leads to a 1.5-fold decrease in burst size; results not shown), and the increase in production rate

268 with virion volume is steeper (the largest viruses create virion volume ~700x faster than the
269 smallest viruses; results not shown). These difference in scaling when using virus genome size
270 vs. virion volume as the predictor are expected, because the genome is a smaller proportion of
271 total virion volume for larger viruses (discussed further in the section *Are larger viruses more*
272 *persistent in the environment?*). An important question for future research is how resource
273 limitation affects these relationships. Nutrient or light limitation have been shown to reduce
274 burst size and lengthen latent period (Wilson et al. 1996, Maat and Brussard 2016,
275 Thamatrakoln et al. 2019), but the data analyzed here are from experiments under resource-
276 replete conditions. It is possible that the advantage of large genome size is greater under
277 resource limitation, due to a greater control of rate-limiting metabolic reactions.

278

279 **Do larger viruses have broader host ranges?**

280 Relatively large viruses could be favored in competition with smaller viruses if a larger
281 genome size is associated with a broader host range (Appendix S3; Chow and Suttle 2015).
282 There is substantial evidence that the ability to attach to host cells plays a major role in defining
283 viral host range (Tétart et al. 1996, Tarutani et al. 2006, Stoddard et al. 2007, Lin et al. 2012, Le
284 et al. 2013), and laboratory experiments often find that hosts evolve resistance by limiting
285 attachment (Lenski 1988, Stoddard et al. 2007). Therefore, virus size may be correlated with
286 host range if having more genes facilitates attachment to a broader range of receptors. For
287 example, the large myovirus phi92 possesses a ‘Swiss army knife’ of multiple tail fibers and/or
288 spikes that appears to facilitate a relatively broad host range encompassing diverse *Escherichia*
289 *coli* and *Salmonella* strains (Schwarzer et al. 2012). In addition, if the largest viruses are typically
290 ingested by their hosts then they may have a broader host range than smaller non-ingested

291 viruses, due to the fact that ingestion of prey tends to be a less specific interaction than ligand-
292 receptor binding.

293 Although attachment is known to be important in defining host range, in some cases
294 viruses can attach with equal or lesser efficiency to related strains or taxa that do not yield
295 productive infections (Samimi and Drews 1978, Thomas et al. 2011, Yau et al. 2018).
296 Presumably the infections were not productive in these cases because of many processes
297 downstream of attachment that can limit infection success, such as successful entry into the host,
298 intracellular host defense mechanisms, and effective meshing with host replication and
299 translation machinery (Samson et al. 2013). Furthermore, attaching to a relatively narrow range
300 of cell types in the environment can be adaptive if broader attachment results in a loss of virions
301 to hosts that cannot be infected as productively (Heineman et al. 2008). Therefore, the ability
302 to create productive infections once attached may play a large role in defining host range, and
303 viruses with more genes that provide greater autonomy during infection, via control of
304 replication, transcription, translation, or metabolism, or by evading host defenses, may achieve
305 productive infections in a broader range of hosts.

306 To assess whether there is an association between genome size and host range we re-
307 analyzed data from two studies of marine phages. Holmfeldt and colleagues characterized a
308 taxonomically diverse collection of 40 phages isolated on 21 strains of the marine bacterium
309 *Cellulophaga baltica* (Holmfeldt et al. 2007, Holmfeldt et al. 2016, Sulcius and Holmfeldt 2016).
310 Across these phages there is an overall positive correlation between host range and genome
311 size, if host range is quantified as the proportion of 21 *Cellulophaga* strains infected (Fig. 3A; r
312 = 0.49, $p = 0.001$). We also quantified host range in a way that incorporates phylogenetic
313 relatedness of the host strains, using the summed branch lengths of the infected strains,

314 calculated from a phylogeny estimated from ribosomal internal transcribed spacer (ITS)
315 sequences; this yielded similar results (results not shown). A positive relationship also appears
316 to occur within phage families, with larger isolates of myovirus, siphovirus, and podovirus
317 having a greater host range than smaller isolates within the same groups (Fig. 3A). However,
318 when phage family and phage genus (as classified by Holmfeldt et al. [2016]) are both included
319 as a random effects in a mixed model, in order to account for phylogenetic non-independence
320 in host range (Felsenstein 1985), the effect of host genome size is less clear ($\chi_1 = 2.45$, $p = 0.12$).
321 This suggests that an even greater phylogenetic diversity of viruses may be needed to robustly
322 test such relationships using a comparative approach. Wichels et al. (1998) characterized 22
323 phages from the North Sea that infect the bacteria *Pseudoalteromonas*. Across the phages in this
324 study there is also a positive correlation between genome size and host range ($r = 0.79$, $p <$
325 0.001), and evidence for such a relationship remains after taxonomic random effects are
326 included in a generalized additive mixed model ($\chi_{1,2} = 7.2$, $p = 0.007$; taxonomic terms include
327 family, morphotype, and species as defined by the authors).

328 In sum, it may be the case that viruses with larger genomes tend to infect a broader range
329 of hosts, and future analyses from diverse host-virus systems would help test the generality of
330 this pattern. At the same time, it is noteworthy that among *Cellulophaga* phages the smallest
331 phage family, the Microviridae, exhibit relatively broad host range on average (Fig. 3A). A large
332 study of *Vibrio* phages also found that small phages, which the authors classified as
333 Autolykiviridae, had broader host ranges than larger Caudovirales (Kauffman et al. 2018). Future
334 work incorporating a quantitative metric of viral fitness on each host strain would help test
335 whether small, broad-range viruses suffer a cost of lower fitness on each individual host strain
336 (Jover et al. 2013, Record et al. 2016). Tradeoffs affecting viral traits, including those related to

337 size and those orthogonal to size, are likely multidimensional (Goldhill and Turner 2014), and
338 therefore it will be important to measure multiple traits on a diversity of viruses to better
339 understand the constraints on viral evolution.

340

341 **Are larger viruses more persistent in the environment?**

342 The rate at which free virions are lost from a viral population is as important for fitness as
343 adsorption rate, burst size, or host range (eqn. 1). However, the effects of virus size on loss rates
344 are poorly known. Decay of phage infectivity in marine systems has been shown to be
345 influenced by sunlight, adsorption to particles, high molecular weight dissolved material such
346 as enzymes, and ingestion by protists (Suttle and Chen 1992, Noble and Furhman 1997).
347 Although a number of studies have estimated decay rates and how they vary across
348 environmental gradients, we are not aware of studies that look at whether these rates vary
349 systematically with size. Heldal and Bratbaak (1991) noted that viruses > 60 nm disappeared
350 more slowly when viral production was halted with cyanide, but they presented no quantitative
351 data.

352 The physical forces that affect virion stability likely vary with size. For viruses with larger
353 double-stranded genomes the capsid can be highly pressurized due to the dense packaging of
354 negatively charged, dehydrated, curved nucleic acids (Purohit et al. 2003, Li et al. 2008,
355 Molineux and Panja 2013). In a comparative study of coliphages, De Paepe and Taddei (2006)
356 found that phages with a faster multiplication rate in culture had a faster decay rate as well.
357 Faster decay was also associated with a higher nucleotide packaging density and a lower
358 surfacic mass (capsid molecular weight per capsid surface area), suggesting that greater pressure

359 makes capsids less stable, and this can be partially mitigated by increased capsid thickness. A
360 re-analysis of their data shows that virus diameter is also negatively correlated with decay rate
361 ($r = -0.64$; mixed model with virus family random effect – $F_{1,13} = 9.1$, $p = 0.01$; Fig. 4A), which
362 could be due to larger phages having lower packaging density, higher surfacic mass, or other
363 causes.

364 We have compiled measurements of genome length and virion dimensions for 193 viruses
365 (Table S3; Methods S1). Among dsDNA viruses infecting unicellular organisms, the fraction of
366 the virion volume occupied by the viral genome declines systematically with increasing virion
367 size (Fig. 4B), although there are notable differences among virus types. The tailless viruses
368 infecting prokaryotes tend to have a lower fractional volume than other dsDNA viruses of the
369 same size, and genome fractional volume declines steeply with increasing virion size for this
370 group and for the eukaryote-infecting dsDNA viruses, which vary more than tenfold in diameter.
371 In contrast, genome fractional volume of the tailed viruses infecting prokaryotes (members of
372 the family *Caudovirales*) is uniformly high and weakly correlated with virion size. Regression
373 analyses indicate that the slope of $\log(\text{genome fractional volume})$ vs. $\log(\text{equivalent spherical}$
374 $\text{diameter})$ is ~ -1.7 for dsDNA eukaryote viruses and tailless dsDNA viruses infecting prokaryotes,
375 while the slope for tailed phages is -0.24 (Fig. S4A). It is also noteworthy that the largest viruses
376 overlap with small prokaryote and eukaryote cells, both in diameter and genome fractional
377 volume, and that the largest viruses tend to infect phagotrophic eukaryotes.

378 A decline in genome fractional volume with virion size could be driven by selection for
379 virion stability, because the pressure at which a capsid bursts is expected to be inversely
380 proportional to capsid radius (Aznar et al. 2012). If dsDNA viruses generally evolve to have an
381 internal pressure near the burst limit, then the packaging density of the genome would have to

382 decline such that internal pressure is inversely proportional to capsid radius. However, without
383 direct measurements it is unclear whether the observed decline in density is sufficient to
384 equalize the stability of larger and smaller viruses, or whether larger viruses tend to be more or
385 less stable on average. In addition, for tailed dsDNA bacteriophages the injection of the viral
386 genome into the host cell may be driven by high genome packaging density, likely due to
387 hydrodynamic effects of the osmotic imbalance with the host cytoplasm (Molineux and Panja
388 2013). In contrast, eukaryote-infecting viruses and tailless prokaryote viruses often use
389 membrane fusion, endocytosis, or phagocytosis as an entry mechanism, although some have a
390 more phage-like strategy (Nurmemmedov et al. 2007, Wulfmeyer et al. 2012, Mäntynen et al.
391 2019). Therefore, while tailed phages may require dense packaging of nucleic acids, many of
392 the largest eukaryote-infecting viruses may reap little benefit from a pressurized capsid. The
393 presence of a lipid envelope around the capsid may contribute to a lower genome fractional
394 volume for many of the tailless dsDNA prokaryote viruses, but the large difference in fractional
395 volume between these viruses and the tailed phages indicates that the envelope itself is likely
396 not the primary cause (Fig. S4B). The dsRNA viruses may follow a scaling relationship similar
397 to the tailless dsDNA phages, but the number of representatives in the dataset is relatively small
398 (Fig. 4B).

399 Fractional genome volume also declines with virion size for ssRNA and ssDNA viruses,
400 and these two kinds of viruses appear to follow a similar scaling relationship (Fig. 4B). This
401 similarity is also apparent when viruses infecting multicellular organisms are included in the
402 comparison (Fig. S4C). The slope of the relationship is ~ -2.8 for the single-stranded viruses
403 infecting unicells (Fig. S4A). This systematic size scaling may also be due to selection equalizing
404 the stability of larger and smaller viruses, although the scaling relationship and mean fractional

405 volume likely differ between single-stranded viruses and double-stranded viruses due to
406 different physical processes underlying virion assembly and stability (Šiber et al. 2012).

407 Finally, physical instability may not be the primary cause of losses of infectious virions, at
408 least in environments where solar radiation and/or non-specific adsorption are high (Suttle and
409 Chen 1992, Noble and Furhman 1997). Viruses with larger genomes have the capacity to code
410 for and package protective enzymes such as photolyase (Fischer et al. 2014), which could lead
411 to slower decay rates for larger viruses. To understand the consequences of these patterns for
412 viral fitness, and to test whether decay rate generally changes with virus size, future work should
413 investigate decay rates in the laboratory and in natural systems for a broad size range of viruses.

414

415

Synthesis and outlook

416 Here we summarize our findings on the relationships between virus size and important
417 virus traits, and we discuss implications and future research directions.

418 The physics of Brownian motion predicts that smaller viruses should encounter their hosts
419 at a faster rate (Fig. 1A), but observed adsorption rates are often much lower than theoretical
420 contact rates (Fig. 1C), and it is possible that larger viruses have a greater attachment efficiency
421 (Fig. 1D). New measurements of adsorption rates of large viruses are needed to test this
422 possibility. Furthermore, entering the host cell via phagocytosis may be a particularly good
423 strategy for ensuring that encounter leads to infection, but demonstrating this quantitatively will
424 require studies on the mechanism of entry, and efficiency of attachment and entry, for diverse
425 viruses.

426 Burst size is lower for larger viruses (Fig. 2A), which is expected if host materials and
427 energy limit viral production, but the cost is less than would be expected if viral production was
428 inversely proportional to genome size. This is likely due to greater control of viral replication
429 and host physiology by viruses with larger genomes, as evidenced by their greater nucleotide
430 production rate (Fig. 2C). Host range may generally increase with virus size, as observed for two
431 diverse groups of phages infecting aquatic bacteria (Fig. 3), and this may be due to greater
432 autonomy during replication, a greater range of counter-defenses, or ability to attach to a greater
433 diversity of receptors. Finally, decay rate has not been widely studied for viruses with unicellular
434 hosts, but a comparison of coliphages suggests that larger viruses could have a lower decay rate
435 (Fig. 4A). In sum these observations suggest that larger viruses experience reductions in burst
436 size, a modest or negligible reduction in adsorption rate, an increase in host range, and
437 potentially a decline in decay rate. These countervailing selection pressures may explain how
438 viruses of very different size have evolved and can persist when infecting the same host
439 population.

440 Are there particular host traits or environmental conditions that could select for larger or
441 smaller viruses? To address this, we can ask whether particular contexts may change the
442 magnitude or direction of relationships between virus size and different virus traits. For example,
443 are there conditions under which the reduction in burst size with increased virus size is lessened?
444 The data synthesized in Figure 2 come from experiments with resource-replete host cultures,
445 and it is possible that under host resource limitation a greater virus size is more costly (due to
446 less energy and materials available for replication) or less costly (due to greater control of host
447 metabolism). Testing this possibility will require measurements of the infection cycle of diverse
448 viruses under different resource conditions. Although contact rates are predicted to decline for

449 larger viruses due to reduced diffusivity, the magnitude of the decline is somewhat less when
450 hosts are motile or generate feeding currents (Fig. 1A). Therefore, larger viruses may be more
451 common among hosts that are highly motile. Likewise, if phagotrophy is an effective means of
452 entering host cells, for viruses large enough to induce phagotrophy, then the largest viruses may
453 be particularly prevalent among phagotrophic hosts (Fig. 4B).

454 If larger viruses tend to have a broader host range, the benefits of broad host range may be
455 greatest when hosts are at low abundance. In our model of host range evolution, a virus will be
456 able to persist if the sum of its host populations, in the absence of viral mortality, exceeds the
457 minimum persistence threshold S^* (Appendix S3). Therefore, oligotrophic environments may be
458 enriched in larger viruses if smaller viruses with narrower host ranges cannot persist. Low host
459 density is also expected to select for lysogeny (Stewart and Levin 1984, Weitz et al. 2019), and
460 so environments with a greater proportion of lysogenic viruses may also tend to have larger
461 viruses in the lytic fraction. Finally, if larger size is associated with reduced decay rates then this
462 relationship may be steeper under conditions of rapid decay, such as exposure to high insolation,
463 which could select for larger viruses.

464 If we combine several of the conditions that could favor large viruses, it may be that motile,
465 phagotrophic protists with low population densities are particularly likely to host giant viruses.
466 Low population densities are characteristic of the oligotrophic open ocean and other
467 environments with low nutrient or energy supply. These environments are also relatively
468 enriched in motile, phagotrophic eukaryotes, including mixotrophic phytoplankton and
469 heterotrophic protists (Edwards 2019), compared to more productive environments where
470 immotile, non-phagotrophic diatoms often dominate microbial biomass. Therefore, the effects
471 of low resource supply on both population densities and community structure may cause larger

472 viruses to be favored in oligotrophic environments. Testing for patterns in virus size distributions
473 across environmental conditions or host types will require a suite of methods, including
474 substantial new isolation efforts, as well as metagenomic protocols that can capture the full size
475 spectrum of viruses in the environment while quantitatively comparing viruses with RNA,
476 ssDNA, and dsDNA genomes. For example, two studies compared RNA and DNA viral
477 metagenomes in coastal ocean environments in Hawai'i (Steward et al. 2013) and Antarctica
478 (Miranda et al. 2016) and found that the abundance of RNA viruses rivals that of DNA viruses.
479 The RNA viruses were essentially exclusively eukaryote-infecting, while most of the DNA
480 viruses were likely phages. This implies that RNA viruses, which tend to be smaller, are more
481 prevalent than larger DNA viruses among eukaryotic viruses in coastal environments. No
482 comparable studies have been performed in the open ocean, but we predict that in the pool of
483 eukaryote-infecting viruses, larger DNA viruses, and 'giant' *Mimiviridae* in particular, are more
484 prevalent than small ssDNA or ssRNA viruses in open ocean environments that tend to be more
485 oligotrophic. It is less clear whether one should expect the size structure of prokaryote-infecting
486 viruses to vary as much across environmental gradients in the ocean, because the abundance
487 of prokaryotes varies much less than the abundance and biomass of unicellular eukaryotes (Li
488 et al. 2004). A study of virus morphology across ocean regions found little variation in the
489 structure of the bulk viral community, which is thought to be numerically dominated by
490 bacteriophages (Brum et al. 2013). However, the locations compared in this study were open
491 ocean environments that varied little in chlorophyll-a, a proxy for community biomass;
492 comparing these environments to productive coastal locations may show that smaller phages
493 become more prevalent in coastal systems.

494 Compilations of virus isolates across the tree of life show that bacteria and archaea are
495 mainly infected by dsDNA viruses with a range of sizes, while eukaryote viruses primarily have
496 RNA genomes that tend to be small, although there is a substantial minority of eukaryote-
497 infecting DNA viruses that tend to be larger (Koonin et al. 2015, Campillo-Balderas et al. 2015).
498 The genome composition and size distribution of eukaryote viruses may reflect alternative
499 strategies responding to the barrier of the eukaryote nucleus, which restricts access to the host's
500 DNA replication and transcription machinery. Larger DNA viruses typically replicate partially
501 or entirely in the cytoplasm, producing their own replication 'factories', while positive-sense
502 single-stranded RNA viral genomes can immediately act as a template for translation (Schmid
503 et al. 2014, Koonin et al. 2015). In our analyses of burst size and decay rate we have treated
504 viruses with different genome types as comparable data points along the virus size spectrum
505 (Figs. 2,4), but future work may consider whether there are important trait or niche differences
506 between these groups that are not explained by size alone. It could also be the case that viruses
507 of different size or different genome type differ in evolutionary rates of 'speciation' or extinction,
508 for example if size or genome type affect the probability of host range shifts, or success in
509 coevolutionary arms races with hosts (Lenski and Levin 1985). Effects of size or genome type
510 on diversification rates could vary with host type or environmental conditions, leading to
511 patterns of virus diversity that vary with host type or environment. Future work may address
512 these possibilities by applying macroevolutionary phylogenetic models to diverse viral clades
513 (e.g., Caetano et al. 2018).

514 Finally, we have focused here on lytic viruses, because a substantial number of lytic viruses
515 infecting unicellular aquatic organisms have been isolated and characterized. Selection for a
516 temperate strategy of integrating into the host genome may also lead to important constraints on

517 virus size evolution. The temperate strategy is a form of vertical symbiont transmission and is
518 expected to be selected for when host densities are low (making horizontal transmission less
519 likely) and when the virus presents a low fitness cost or even a benefit (Weitz et al. 2019).
520 Considering the potential costs and benefits of prophage or provirus in the host genome, a larger
521 virus genome will incur greater material and energy costs but will also be able to encode more
522 functions that could benefit the host. Future work may consider how the size distribution of
523 temperate viruses compares to lytic viruses, across environmental gradients or different host
524 characteristics.

525

526

Acknowledgements

527 This work was supported by National Science Foundation awards OCE 15-59356 and RII Track-
528 2 FED 17-36030 (to G.F.S and K.F.E.) and a Simons Foundation Investigator Award in Marine
529 Microbial Ecology and Evolution (to K.F.E.). We thank Marcia Marston for providing information
530 about the size of cyanophage RIM8.

531

532

References

533 Abedon, S. T., Hyman, P., & Thomas, C. (2003). Experimental examination of bacteriophage latent-
534 period evolution as a response to bacterial availability. *Appl. Environ. Microbiol.*, 69(12), 7499–7506.
535 Al-Shayeb, B., Sachdeva, R., Chen, L.X., Ward, F., Munk, P., Devoto, A., Castelle, C.J., Olm, M.R.,
536 Bouma-Gregson, K., Amano, Y. and He, C. (2020). Clades of huge phages from across Earth's
537 ecosystems. *Nature*, 1-7.

538 Aznar, M., Luque, A., & Reguera, D. (2012). Relevance of capsid structure in the buckling and maturation
539 of spherical viruses. *Physical biology*, 9(3), 036003.

540 Birch, E. W., Ruggero, N. A., & Covert, M. W. (2012). Determining host metabolic limitations on viral
541 replication via integrated modeling and experimental perturbation. *PLoS Computational Biology*, 8(10),
542 e1002746.

543 Brown, J. H., Gillooly, J. F., Allen, A. P., Savage, V. M., & West, G. B. (2004). Toward a metabolic theory
544 of ecology. *Ecology*, 85(7), 1771–1789.

545 Brum, J. R., Schenck, R. O., & Sullivan, M. B. (2013). Global morphological analysis of marine viruses
546 shows minimal regional variation and dominance of non-tailed viruses. *The ISME journal*, 7(9), 1738-
547 1751.

548 Caetano, D. S., O'Meara, B. C., & Beaulieu, J. M. (2018). Hidden state models improve state-dependent
549 diversification approaches, including biogeographical models. *Evolution*, 72(11), 2308-2324.

550 Campillo-Balderas, J. A., Lazcano, A., & Becerra, A. (2015). Viral genome size distribution does not
551 correlate with the antiquity of the host lineages. *Frontiers in Ecology and Evolution*, 3, 143.

552 Chow, C. E. T., & Suttle, C. A. (2015). Biogeography of viruses in the sea. *Annual review of virology*, 2,
553 41-66.

554 Chrzanowski, T. H., & Šimek, K. (1990). Prey-size selection by freshwater flagellated protozoa. *Limnology
555 and Oceanography*, 35(7), 1429–1436.

556 Cui, J., Schlub, T.E. and Holmes, E.C., 2014. An allometric relationship between the genome length and
557 virion volume of viruses. *Journal of Virology*, 88(11), pp.6403-6410.

558 De Paepe, M., & Taddei, F. (2006). Viruses' life history: towards a mechanistic basis of a trade-off
559 between survival and reproduction among phages. *PLoS Biology*, 4(7), e193.

560 Devoto, A.E., Santini, J.M., Olm, M.R., Anantharaman, K., Munk, P., Tung, J., Archie, E.A., Turnbaugh,
561 P.J., Seed, K.D., Blekhman, R. and Aarestrup, F.M. (2019). Megaphages infect *Prevotella* and variants
562 are widespread in gut microbiomes. *Nature Microbiology*, 4(4), 693.

563 Edwards, K. F., & Steward, G. F. (2018). Host traits drive viral life histories across phytoplankton viruses.
564 *The American Naturalist*, 191(5), 566–581.

565 Edwards, K. F., Thomas, M. K., Klausmeier, C. A., & Litchman, E. (2012). Allometric scaling and
566 taxonomic variation in nutrient utilization traits and maximum growth rate of phytoplankton.
567 *Limnology and Oceanography*, 57(2), 554–566.

568 Epstein, S. S., & Shiaris, M. P. (1992). Size-selective grazing of coastal bacterioplankton by natural
569 assemblages of pigmented flagellates, colorless flagellates, and ciliates. *Microbial Ecology*, 23(3), 211–
570 225.

571 Felsenstein, J. (1985). Phylogenies and the comparative method. *The American Naturalist*, 125(1), 1–15.

572 Finkel, Z. V, & Irwin, A. J. (2001). Light absorption by phytoplankton and the filter amplification
573 correction: cell size and species effects. *Journal of Experimental Marine Biology and Ecology*, 259(1),
574 51–61.

575 Fischer, M. G., Allen, M. J., Wilson, W. H., & Suttle, C. A. (2010). Giant virus with a remarkable
576 complement of genes infects marine zooplankton. *Proceedings of the National Academy of*
577 *Sciences*, 107(45), 19508-19513.

578 Fischer, M. G., Kelly, I., Foster, L. J., & Suttle, C. A. (2014). The virion of *Cafeteria roenbergensis* virus
579 (CroV) contains a complex suite of proteins for transcription and DNA repair. *Virology*, 466, 82-94.

580 Fuchs, H. L., & Franks, P. J. S. (2010). Plankton community properties determined by nutrients and size-
581 selective feeding. *Marine Ecology Progress Series*, 413, 1–15.

582 Goldhill, D. H., & Turner, P. E. (2014). The evolution of life history trade-offs in viruses. *Current opinion*
583 *in virology*, 8, 79-84.

584 Heineman, R. H., Springman, R., & Bull, J. J. (2008). Optimal foraging by bacteriophages through host
585 avoidance. *The American Naturalist*, 171(4), E149–E157.

586 Heldal, M., & Bratbak, G. (1991). Production and decay of viruses in aquatic environments. *Mar. Ecol.*
587 *Prog. Ser.*, 72(3), 205–212.

588 Holen, D. A., & Boraas, M. E. (1991). The feeding behavior of *Spumella* sp. as a function of particle size:
589 Implications for bacterial size in pelagic systems. *Hydrobiologia*, 220(1), 73–88.

590 Holmfeldt, K., Middelboe, M., Nybroe, O., & Riemann, L. (2007). Large variabilities in host strain
591 susceptibility and phage host range govern interactions between lytic marine phages and their
592 *Flavobacterium* hosts. *Appl. Environ. Microbiol.*, 73(21), 6730–6739.

593 Holmfeldt, K., Solonenko, N., Howard-Varona, C., Moreno, M., Malmstrom, R. R., Blow, M. J., & Sullivan,
594 M. B. (2016). Large-scale maps of variable infection efficiencies in aquatic Bacteroidetes phage-host
595 model systems. *Environmental Microbiology*, 18(11), 3949–3961.

596 Holmfeldt, K., Solonenko, N., Shah, M., Corrier, K., Riemann, L., VerBerkmoes, N. C., & Sullivan, M. B.
597 (2013). Twelve previously unknown phage genera are ubiquitous in global oceans. *Proceedings of*
598 *the National Academy of Sciences*, 110(31), 12798–12803.

599 Jover, L. F., Cortez, M. H., & Weitz, J. S. (2013). Mechanisms of multi-strain coexistence in host–phage
600 systems with nested infection networks. *Journal of Theoretical Biology*, 332, 65–77.

601 Karp-Boss, L., Boss, E., & Jumars, P. A. (1996). Nutrient fluxes to planktonic osmotrophs in the presence
602 of fluid motion. *Oceanography and Marine Biology*, 34, 71–108.

603 Kauffman, K.M., Hussain, F.A., Yang, J., Arevalo, P., Brown, J.M., Chang, W.K., VanInsberghe, D.,
604 Elsherbini, J., Sharma, R.S., Cutler, M.B. and Kelly, L. (2018). A major lineage of non-tailed dsDNA
605 viruses as unrecognized killers of marine bacteria. *Nature*, 554(7690), 118.

606 Kiørboe, T. (2008). *A mechanistic approach to plankton ecology*. Princeton University Press.

607 Koonin, E. V. & Yutin, N. (2019). Evolution of the large nucleocytoplasmic DNA viruses of eukaryotes
608 and convergent origins of viral gigantism. *Adv. Virus Res*, 103, 167–202.

609 Langlois, V. J., Andersen, A., Bohr, T., Visser, A. W., & Kiørboe, T. (2009). Significance of swimming and
610 feeding currents for nutrient uptake in osmotrophic and interception-feeding flagellates. *Aquatic*
611 *Microbial Ecology*, 54(1), 35–44.

612 Le, S., He, X., Tan, Y., Huang, G., Zhang, L., Lux, R., Shi, W. and Hu, F. (2013). Mapping the tail fiber
613 as the receptor binding protein responsible for differential host specificity of *Pseudomonas aeruginosa*
614 bacteriophages PaP1 and JG004. *PLoS One*, 8(7), e68562.

615 Lenski, R. E., & Levin, B. R. (1985). Constraints on the coevolution of bacteria and virulent phage: a
616 model, some experiments, and predictions for natural communities. *The American Naturalist*, 125(4),
617 585-602.

618 Lenski, R. E. (1988). Experimental studies of pleiotropy and epistasis in *Escherichia coli*. I. Variation in
619 competitive fitness among mutants resistant to virus T4. *Evolution*, 42(3), 425–432.

620 Levin, B. R., Stewart, F. M., & Chao, L. (1977). Resource-limited growth, competition, and predation: a
621 model and experimental studies with bacteria and bacteriophage. *The American Naturalist*, 111(977),
622 3–24.

623 Li, W. K., Head, E. J., & Harrison, W. G. (2004). Macroecological limits of heterotrophic bacterial
624 abundance in the ocean. *Deep Sea Research Part I: Oceanographic Research Papers*, 51(11), 1529-
625 1540.

626 Li, Z., Wu, J., & Wang, Z. G. (2008). Osmotic pressure and packaging structure of caged
627 DNA. *Biophysical journal*, 94(3), 737-746.

628 Lin, T.-Y., Lo, Y.-H., Tseng, P.-W., Chang, S.-F., Lin, Y.-T., & Chen, T.-S. (2012). A T3 and T7 recombinant
629 phage acquires efficient adsorption and a broader host range. *PLoS One*, 7(2), e30954.

630 Maat, D. S., & Brussaard, C. P. D. (2016). Both phosphorus-and nitrogen limitation constrain viral
631 proliferation in marine phytoplankton. *Aquatic Microbial Ecology*, 77(2), 87–97.

632 Mäntynen, S., Sundberg, L. R., Oksanen, H. M., & Poranen, M. M. (2019). Half a century of research on
633 Membrane-Containing bacteriophages: bringing new concepts to modern virology. *Viruses*, 11(1), 76.

634 Miranda, J. A., Culley, A. I., Schvarcz, C. R., & Steward, G. F. (2016). RNA viruses as major contributors
635 to Antarctic viroplankton. *Environmental microbiology*, 18(11), 3714-3727.

636 Molineux, I. J., & Panja, D. (2013). Popping the cork: mechanisms of phage genome ejection. *Nature*
637 *Reviews Microbiology*, 11(3), 194-204.

638 Murray, A. G., & Jackson, G. A. (1992). Viral dynamics: a model of the effects of size, shape, motion and
639 abundance of single-celled planktonic organisms and other particles. *Marine Ecology Progress Series*,
640 103–116.

641 Noble, R. T., & Fuhrman, J. A. (1997). Virus decay and its causes in coastal waters. *Appl. Environ.*
642 *Microbiol.*, 63(1), 77–83.

643 Nurmammedov E, Castelnovo M, Catalano CE, Evilevitch A. (2007). Biophysics of viral infectivity:
644 matching genome length with capsid size. *Q Rev Biophys*, 40, 327–356.

645 Purohit, P. K., Kondev, J., & Phillips, R. (2003). Mechanics of DNA packaging in viruses. *Proceedings of*
646 *the National Academy of Sciences*, 100(6), 3173-3178.

647 Rodrigues, R. A. L., Abrahão, J. S., Drumond, B. P., & Kroon, E. G. (2016). Giants among larges: how
648 gigantism impacts giant virus entry into amoebae. *Current Opinion in Microbiology*, 31, 88–93.

649 Samimi, B., & Drews, G. (1978). Adsorption of cyanophage AS-1 to unicellular cyanobacteria and
650 isolation of receptor material from *Anacystis nidulans*. *Journal of Virology*, 25(1), 164–174.

651 Samson, J. E., Magadán, A. H., Sabri, M., & Moineau, S. (2013). Revenge of the phages: defeating
652 bacterial defences. *Nature Reviews Microbiology*, 11(10), 675.

653 Schmid, M., Speiseder, T., Dobner, T., & Gonzalez, R. A. (2014). DNA virus replication
654 compartments. *Journal of virology*, 88(3), 1404-1420.

655 Schwartz, M. (1976). The adsorption of coliphage lambda to its host: effect of variations in the surface
656 density of receptor and in phage-receptor affinity. *Journal of Molecular Biology*, 103(3), 521–536.

657 Schwarzer, D., Buettner, F.F., Browning, C., Nazarov, S., Rabsch, W., Bethe, A., Oberbeck, A., Bowman,
658 V.D., Stummeyer, K., Mühlenhoff, M. and Leiman, P.G. (2012). A multivalent adsorption apparatus
659 explains the broad host range of phage phi92: a comprehensive genomic and structural analysis.
660 *Journal of Virology*, 86(19), 10384–10398.

661 Sharon, I., Battchikova, N., Aro, E.M., Giglione, C., Meinnel, T., Glaser, F., Pinter, R.Y., Breitbart, M.,
662 Rohwer, F. and Béja, O. (2011). Comparative metagenomics of microbial traits within oceanic viral
663 communities. *The ISME Journal*, 5(7), 1178.

664 Shimeta, J. (1993). Diffusional encounter of submicrometer particles and small cells by suspension
665 feeders. *Limnol. Oceanogr.*, 38, 456–465.

666 Shinn, G. L., & Bullard, B. L. (2018). Ultrastructure of Meelsvirus: A nuclear virus of arrow worms (phylum
667 Chaetognatha) producing giant “tailed” virions. *PloS One*, 13(9), e0203282.

668 Šiber, A., Božič, A. L., & Podgornik, R. (2012). Energies and pressures in viruses: contribution of
669 nonspecific electrostatic interactions. *Physical chemistry chemical physics*, 14(11), 3746-3765.

670 Šimek, K., & Chrzanowski, T. H. (1992). Direct and indirect evidence of size-selective grazing on pelagic
671 bacteria by freshwater nanoflagellates. *Appl. Environ. Microbiol.*, 58(11), 3715–3720.

672 Steward, G. F., Culley, A. I., Mueller, J. A., Wood-Charlson, E. M., Belcaid, M., & Poisson, G. (2013).
673 Are we missing half of the viruses in the ocean?. *The ISME journal*, 7(3), 672-679.

674 Stoddard, L. I., Martiny, J. B. H., & Marston, M. F. (2007). Selection and characterization of cyanophage
675 resistance in marine *Synechococcus* strains. *Appl. Environ. Microbiol.*, 73(17), 5516–5522.

676 Storms, Z. J., & Sauvageau, D. (2015). Modeling tailed bacteriophage adsorption: Insight into
677 mechanisms. *Virology*, 485, 355–362.

678 Šulčius, S., & Holmfeldt, K. (2016). Viruses of microorganisms in the Baltic Sea: current state of research
679 and perspectives. *Marine Biology Research*, 12(2), 115–124.

680 Suttle, C. A., & Chen, F. (1992). Mechanisms and rates of decay of marine viruses in seawater. *Appl.*
681 *Environ. Microbiol.*, 58(11), 3721–3729.

682 Talmy, D., Beckett, S. J., Zhang, A. B., Taniguchi, D. A. A., Weitz, J. S., & Follows, M. J. (2019).
683 Contrasting controls on microzooplankton grazing and viral infection of microbial prey. *Front. Mar.*
684 *Sci*, 6, 182.

685 Tarutani, K., Nagasaki, K., & Yamaguchi, M. (2006). Virus adsorption process determines virus
686 susceptibility in *Heterosigma akashiwo* (Raphidophyceae). *Aquatic Microbial Ecology*, 42(3), 209–
687 213.

688 Tétart, F., Repoila, F., Monod, C., & Krisch, H. M. (1996). Bacteriophage T4 host range is expanded by
689 duplications of a small domain of the tail fiber adhesin. Elsevier.

690 Thamtrakoln, K., Talmy, D., Haramaty, L., Maniscalco, C., Latham, J.R., Knowles, B., Natale, F., Coolen,
691 M.J., Follows, M.J. and Bidle, K.D. (2019). Light regulation of coccolithophore host–virus interactions.
692 *New Phytologist*, 221(3), 1289–1302.

693 Thingstad, T. F., Våge, S., Storesund, J. E., Sandaa, R.-A., & Giske, J. (2014). A theoretical analysis of how
694 strain-specific viruses can control microbial species diversity. *Proceedings of the National Academy*
695 *of Sciences*, 111(21), 7813–7818.

696 Thomas, R., Grimsley, N., Escande, M., Subirana, L., Derelle, E., & Moreau, H. (2011). Acquisition and
697 maintenance of resistance to viruses in eukaryotic phytoplankton populations. *Environmental*
698 *Microbiology*, 13(6), 1412–1420.

699 Tilman, D. (1982). *Resource competition and community structure*. Princeton university press.

700 Tomaru, Y., Mizumoto, H., Takao, Y., & Nagasaki, K. (2009). Co-occurrence of DNA-and RNA-viruses
701 infecting the bloom-forming dinoflagellate, *Heterocapsa circularisquama*, on the Japan coast.
702 *Plankton and Benthos Research*, 4(4), 129–134.

703 Wang, N., Dykhuizen, D. E., & Slobodkin, L. B. (1996). The evolution of phage lysis timing. *Evolutionary*
704 *Ecology*, 10(5), 545–558.

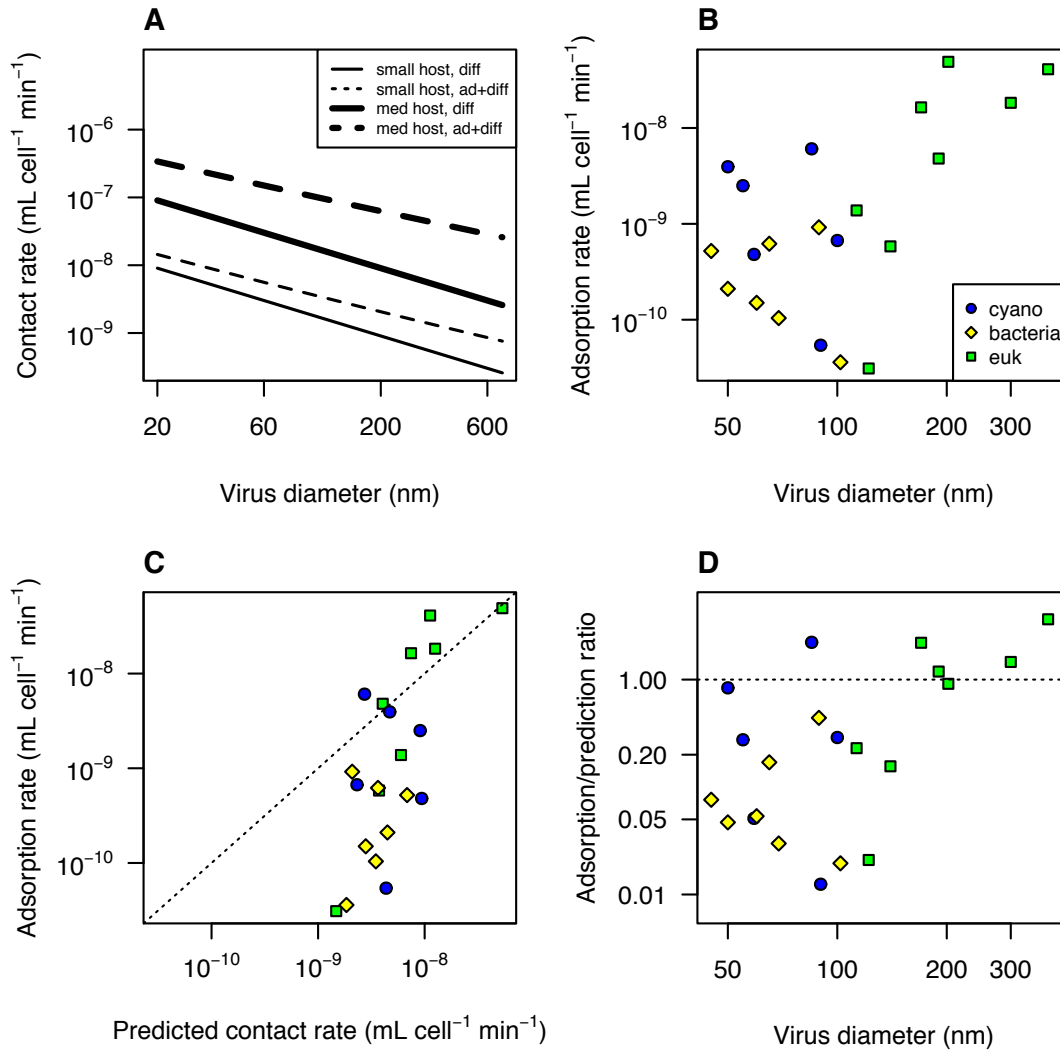
705 Weitz, J. S., Li, G., Gulbudak, H., Cortez, M. H., & Whitaker, R. J. (2019). Viral invasion fitness across a
706 continuum from lysis to latency. *Virus evolution*, 5(1), vez006.

707 Wichels, A., Biel, S. S., Gelderblom, H. R., Brinkhoff, T., Muyzer, G., & Schütt, C. (1998). Bacteriophage
708 diversity in the North Sea. *Appl. Environ. Microbiol.*, 64(11), 4128–4133.

709 Wickham, T. J., Granados, R. R., Wood, H. A., Hammer, D. A., & Shuler, M. L. (1990). General analysis
710 of receptor-mediated viral attachment to cell surfaces. *Biophysical Journal*, 58(6), 1501–1516.

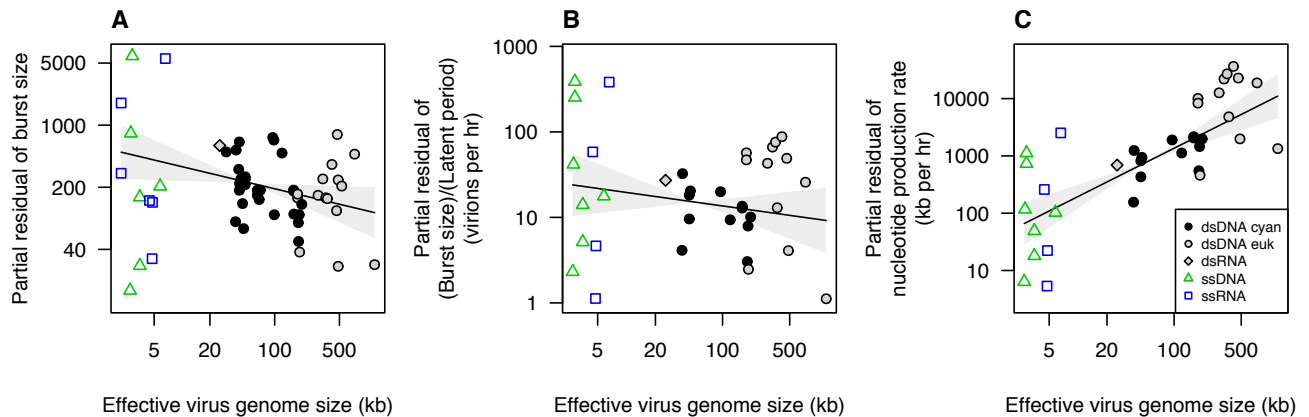
711 Wilhelm, S.W., Bird, J.T., Bonifer, K.S., Calfee, B.C., Chen, T., Coy, S.R., Gainer, P.J., Gann, E.R.,
712 Heatherly, H.T., Lee, J. and Liang, X., 2017. A student's guide to giant viruses infecting small
713 eukaryotes: from Acanthamoeba to Zooxanthellae. *Viruses*, 9(3), 46.

- 714 Wilson, W. H., Carr, N. G., & Mann, N. H. (1996). The effect of phosphate status on the kinetics of
715 cyanophage infection in the oceanic cyanobacterium *Synechococcus* sp. WH7803. *Journal of*
716 *Phycology*, 32(4), 506–516.
- 717 Wulfmeyer, T., Polzer, C., Hiepler, G., Hamacher, K., Shoeman, R., Dunigan, D.D., Van Etten, J.L.,
718 Lolicato, M., Moroni, A., Thiel, G. and Meckel, T. (2012). Structural organization of DNA in chlorella
719 viruses. *PLoS One*, 7(2).
- 720 Yau, S., Caravello, G., Fonvieille, N., Desgranges, É., Moreau, H., & Grimsley, N. (2018). Rapidity of
721 genomic adaptations to prasinovirus infection in a marine microalga. *Viruses*, 10(8), 441.
- 722 You, L., Suthers, P. F., & Yin, J. (2002). Effects of *Escherichia coli* physiology on growth of phage T7 in
723 vivo and in silico. *Journal of Bacteriology*, 184(7), 1888–1894.

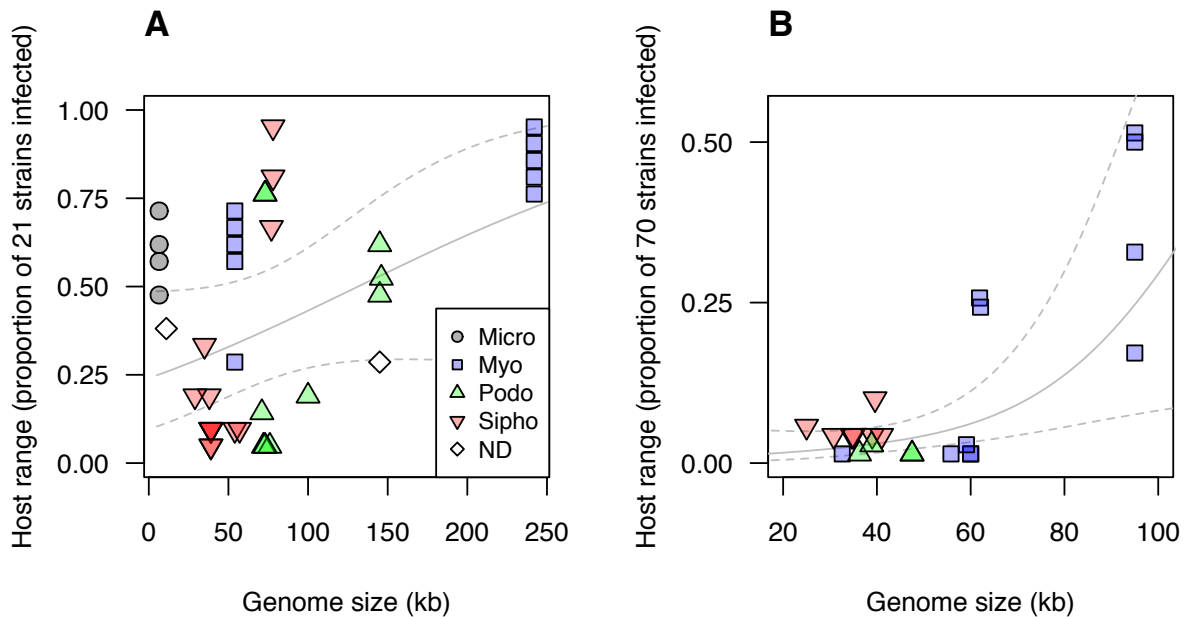


724 **Figure 1.** Model predictions and observations of contact rate and adsorption rate. (A) Predicted contact
 725 rate as a function of virus size. The ‘small host’ lines correspond to a host with diameter $1 \mu\text{m}$ and
 726 swimming speed $10 \mu\text{m s}^{-1}$, and the ‘medium host’ lines correspond to a host with diameter $10 \mu\text{m}$ and
 727 swimming speed $100 \mu\text{m s}^{-1}$. The solid lines are the pure diffusion prediction (no advection), and the
 728 dashed lines are for swimming hosts (advection+diffusion). (B) Observed adsorption rates for viruses of
 729 aquatic bacteria, phytoplankton, and the protist *Cafeteria roenbergensis* (Table S1; Methods S1). (C)
 730 Observed rates vs. theoretical predictions described in Methods S1. (D) Observed adsorption rate, relative
 731 to the theoretical maximum contact rate, as a function of virus size. ‘cyano’ = virus infecting

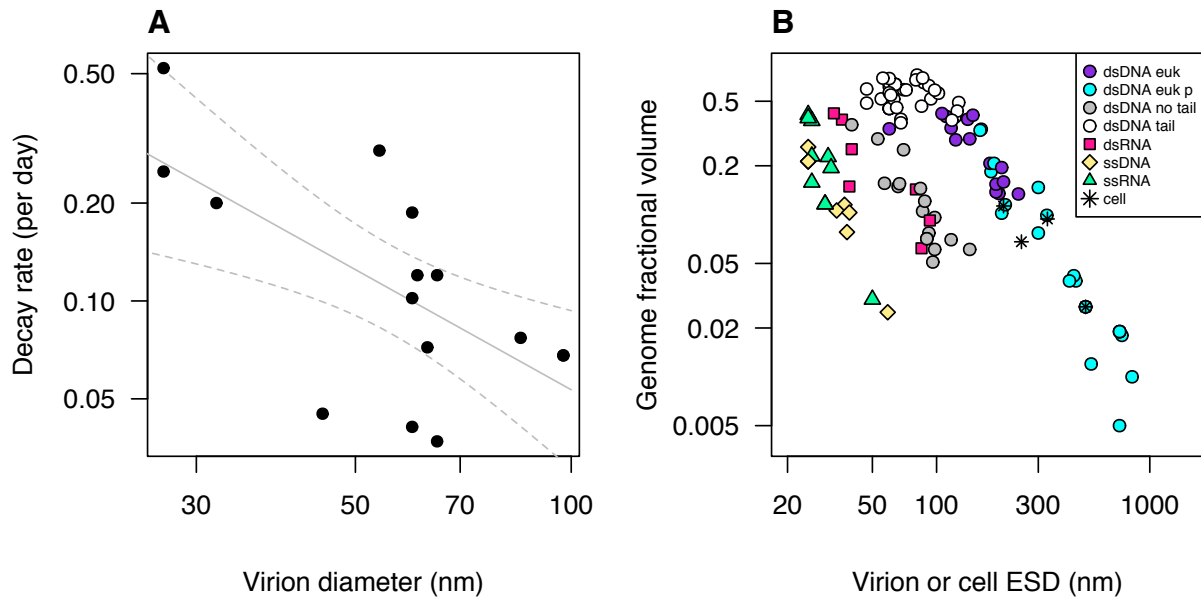
732 cyanobacterium, 'bacteria' = virus infecting heterotrophic bacterium, 'euk' = virus infecting unicellular
733 eukaryote.



734 **Figure 2.** Burst size and production rates as a function of virus genome size for viruses of phytoplankton
735 and the protist *Cafeteria roenbergensis*. (A) Burst size vs. virus genome size. Partial residual burst size is
736 plotted, which removes variation in burst size explained by host genome size. Effective virus genome
737 size is plotted, which divides genome size by 2 for single-stranded viruses. (B) Virion production rate,
738 (burst size)/(latent period), vs. virus genome size. Partial residual production rate is plotted, which
739 removes variation explained by host growth rate. (C) Nucleotide production rate (kb per hr) vs. virus
740 genome size. Partial residual production rate is plotted, which removes variation explained by host
741 growth rate. Plotted lines are fitted smoothers \pm 95% CI from generalized additive mixed models. 'dsDNA
742 cyan' = dsDNA viruses infecting cyanobacteria; 'dsDNA euk' = dsDNA viruses infecting unicellular
743 eukaryotes. dsRNA, ssDNA, and ssRNA viruses all infect eukaryotes in this dataset. Data and data sources
744 are presented in Table S2 and described in Methods S1.



745 **Figure 3.** Host range vs. genome size in marine bacteriophages. (A) Host range (proportion of 21 strains
 746 infected) vs. genome size for *Cellulophaga baltica* phages (Sulcius and Holmfeldt 2016). (B) Host range
 747 (proportion of 70 strains infected) vs. genome size for *Pseudoalteromonas* phages (Wichels et al. 1998).
 748 Lines depict fitted smoothers and 95% CI from generalized additive mixed models that include taxonomic
 749 random effects to account for related viruses having similar host ranges. 'Micro' = Microviridae, 'Myo' =
 750 Myoviridae, 'Podo', = Podoviridae, 'Sipho' = Siphoviridae, 'ND' = taxonomy not determined. Statistical
 751 methods are described further in Methods S1.



752 **Figure 4.** (A) Decay rate vs. virion diameter, for phages that infect *E. coli* (data from Table 1 in De Paepe
 753 and Taddei 2006). Lines are linear regression fit \pm 95% CI. (B) Genome fractional volume vs. equivalent
 754 spherical diameter, for viruses that infect unicellular organisms, and for four representative cellular
 755 organisms. Genome fractional volume is the estimated nucleic acid volume divided by total virion
 756 volume. Cell or virion volumes were estimated from reported outer dimensions (including outer envelope,
 757 if present, but excluding tails or fibrils) using volume formulae for simplified approximate shapes as
 758 indicated in Table S3. Nucleic acid volume is estimated as volume of a cylinder with diameter being
 759 2.37 nm for double-stranded nucleic acid and 1.19 nm for single-stranded and 0.34 nm per nt or bp.
 760 'dsDNA euk' = dsDNA viruses infecting non-phagotrophic eukaryotes, 'dsDNA euk p' = dsDNA viruses
 761 infecting phagotrophic eukaryotes, 'dsDNA no tail' = tailless dsDNA viruses infecting prokaryotes,
 762 'dsDNA tail' = tailed dsDNA viruses infecting prokaryotes, 'dsRNA' = dsRNA viruses, 'ssDNA' = ssDNA
 763 viruses, 'ssRNA' = ssRNA viruses, 'cell' = cellular organisms (one archaeon, two bacteria, one eukaryote).
 764 Data and data sources are presented in Table S3 and described in Methods S1.